University of Reading

Recent global and regional trends in burned area and their compensating environmental controls

Article

Published Version

Creative Commons: Attribution 3.0 (CC-BY)

Open access

Forkel, M., Dorigo, W., Lasslop, G., Chuvieco, E., Hantson, S., Heil, A., Teubner, I., Thonicke, K. and Harrison, S. P. ORCID: https://orcid.org/0000-0001-5687-1903 (2019) Recent global and regional trends in burned area and their compensating environmental controls. Environmental Research Communications, 1 (5). 051005. ISSN 2515-7620 doi: 10.1088/2515-7620/ab25d2 Available at https://centaur.reading.ac.uk/84779/

It is advisable to refer to the publisher's version if you intend to cite from the work. See Guidance on citing.

To link to this article DOI: http://dx.doi.org/10.1088/2515-7620/ab25d2

Publisher: IOP Science

All outputs in CentAUR are protected by Intellectual Property Rights law, including copyright law. Copyright and IPR is retained by the creators or other copyright holders. Terms and conditions for use of this material are defined in the End User Agreement.

University of Reading

www.reading.ac.uk/centaur

CentAUR

Central Archive at the University of Reading

Reading's research outputs online

Environmental Research Communications

LETTER • OPEN ACCESS

Recent global and regional trends in burned area and their compensating environmental controls

To cite this article: Matthias Forkel *et al* 2019 *Environ. Res. Commun.* **1** 051005

View the article online for updates and enhancements.

This content was downloaded from IP address 86.159.85.189 on 06/07/2019 at 14:50

Environmental Research Communications

LETTER

Recent global and regional trends in burned area and their compensating environmental controls

Matthias Forkel[1], **Wouter Dorigo**[1], **Gitta Lasslop**[2], **Emilio Chuvieco**[3], **Stijn Hantson**[4], **Angelika Heil**[5], **Irene Teubner**[1], **Kirsten Thonicke**[6] and **Sandy P Harrison**[7]

[1] Climate and Environmental Remote Sensing Group, Department of Geodesy and Geoinformation, Technische Universität Wien, Vienna, Austria
[2] Senckenberg Biodiversity and Climate Research Centre, Frankfurt am Main, Germany
[3] Environmental Remote Sensing Research Group, Department of Geology, Geography and the Environment, Universidad de Alcalá, Alcalá de Henares, Spain
[4] Geospatial Data Solutions Center, University of California, Irvine, United States of America
[5] Max Planck Institute for Chemistry, Mainz, Germany
[6] Potsdam Institute for Climate Impact Research, Potsdam, Germany
[7] Department of Geography and Environmental Science, The University of Reading, United Kingdom

E-mail: matthias.forkel@geo.tuwien.ac.at

Keywords: fire, greening, VOD, FAPAR, fuel, dynamic global vegetation models, multi-temporal trend analysis

Supplementary material for this article is available online

OPEN ACCESS

RECEIVED
1 April 2019

REVISED
25 April 2019

ACCEPTED FOR PUBLICATION
30 May 2019

PUBLISHED
7 June 2019

Original content from this work may be used under the terms of the Creative Commons Attribution 3.0 licence.

Any further distribution of this work must maintain attribution to the author(s) and the title of the work, journal citation and DOI.

Abstract

The apparent decline in the global incidence of fire between 1996 and 2015, as measured by satellite-observations of burned area, has been related to socioeconomic and land use changes. However, recent decades have also seen changes in climate and vegetation that influence fire and fire-enabled vegetation models do not reproduce the apparent decline. Given that the satellite-derived burned area datasets are still relatively short (<20 years), this raises questions both about the robustness of the apparent decline and what causes it. We use two global satellite-derived burned area datasets and a data-driven fire model to (1) assess the spatio-temporal robustness of the burned area trends and (2) to relate the trends to underlying changes in temperature, precipitation, human population density and vegetation conditions. Although the satellite datasets and simulation all show a decline in global burned area over ~20 years, the trend is not significant and is strongly affected by the start and end year chosen for trend analysis and the year-to-year variability in burned area. The global and regional trends shown by the two satellite datasets are poorly correlated for the common overlapping period (2001–2015) and the fire model simulates changes in global and regional burned area that lie within the uncertainties of the satellite datasets. The model simulations show that recent increases in temperature would lead to increased burned area but this effect is compensated by increasing wetness or increases in population, both of which lead to declining burned area. Increases in vegetation cover and density associated with recent greening trends lead to increased burned area in fuel-limited regions. Our analyses show that global and regional burned area trends result from the interaction of compensating trends in controls of wildfire at regional scales.

1. Introduction

Despite the occurrence of major catastrophic wildfires in recent years (Cruz *et al* 2012, Dennison *et al* 2014, Stephens *et al* 2014, Bowman *et al* 2017), total global burned area (BA) apparently declined between 1996 and 2015 (Van Lierop *et al* 2015, Doerr and Santín 2016, Andela *et al* 2017). This finding is based on satellite-derived burned area data such as from the Global Fire Emissions Database (GFED) (Giglio *et al* 2013). GFED extends burned area estimates from the MODIS sensor (Moderate-Resolution Imaging Spectroradiometer, mid-2000 to

© 2019 The Author(s). Published by IOP Publishing Ltd

2015) for the period 1996–2000 with active fire hotspots from VIRS (Visible and Infrared Scanner) and ATSR (Along-Track Scanning Radiometer). The merging of the burned area estimates from different sensors likely affects the computation of burned area trends (Giglio *et al* 2013). Other burned area datasets have also been derived from MODIS but using different retrieval algorithms and spatial resolutions (Chuvieco *et al* 2018, Giglio *et al* 2018). Comparisons of these datasets show similar spatial patterns of burning but some large differences in global and regional total burned area (Chuvieco *et al* 2016, 2018, Humber *et al* 2019). Generally, the relatively short period covered (15–20 years) makes it difficult to achieve a robust quantification of burned area trends.

The apparent recent decline in global burned area has been associated to human activities, specifically population growth, agricultural expansion and land-use changes mostly in northern-hemisphere Africa (Andela *et al* 2017). However, the incidence of wildfires is influenced by many factors including climate, ignition sources, and vegetation properties (Bowman *et al* 2009, Krawchuk *et al* 2009, Moritz *et al* 2012, Bistinas *et al* 2014, Knorr *et al* 2014). The impact of changes in climate on fire are obviously regionally specific, although high temperatures and increasing summer drought have been invoked as the cause of recent extreme fire seasons (Holden *et al* 2018, Turco *et al* 2018) and climate change has led to an increase in wildfire season length over large parts of the land area (Jolly *et al* 2015). On the other hand, large parts of the world such as the African Sahel have experienced widespread increases in vegetation cover and above-ground biomass (Liu *et al* 2015, Zhu *et al* 2016, Brandt *et al* 2017) which affects fuel availability and thus likely fire incidence and burned area. The influence of such changes on recent trends in global burned area has yet to be adequately assessed.

Fire-enabled dynamic global vegetation models (DGVMs) explicitly account for the effects of climate, humans and vegetation on fire occurrence and could potentially be used to assess controls on burned area trends (Hantson *et al* 2016). However, state-of-the-art DGVMs do not reproduce the observed decline in global burned area: half of the DGVMs from the Fire Model Intercomparion Project (FireMIP) underestimate the apparent decline in global burned area, while the other half show an increase in global burned area (Andela *et al* 2017). These differences in behaviour suggest that some functional relationships and associated parameterisations are poorly constrained in these models. Indeed, analyses of the FireMIP simulations suggest that, while they represent the climate controls on burned area reasonably well, they underestimate the sensitivity to previous-season plant productivity and have over-simplistic representations of the influence of human activities on burned area (Forkel *et al* 2019). Empirical fire models (Moritz *et al* 2012, Bistinas *et al* 2014, Forkel *et al* 2017) provide an alternative and arguably better approach to reproduce observed fire dynamics and to quantify the relative importance of climate, vegetation and human factors on temporal changes in burned area.

In this paper, we first assess the robustness of trends in global burned area using two data sets and taking into consideration the impact of the sampling period and time series length. We then use a recently developed empirical fire model to analyse the relative importance of recent climate, human population, and vegetation changes on these trends.

2. Data and methods

2.1. Burned area data

We analysed two global burned area satellite datasets:

- GFED4 (Global Fire Emissions Database, version 4, 1996–2015 (Giglio *et al* 2013)), based on MODIS 500 m data and prolonged before 2001 with ATSR and VIRS active fire observations; and
- FireCCI50 (European Space Agency Climate Change Initiative, Fire_CCI, version 50, 2001–2015 (Chuvieco *et al* 2018)), based on MODIS 250 m data.

We simulated burned area using an empirical fire model based on the SOFIA (Satellite Observations for FIre Activity) approach, which estimates monthly burned area from observed time series of land cover, vegetation, climate variables and human population density (Forkel *et al* 2017).

All burned area and ancillary datasets were either obtained at or aggregated to 0.25° x 0.25° spatial resolution.

2.2. Trend analysis

We performed a multi-temporal trend analysis to assess the effects of sampling period, time series length, and year-to-year variability on estimated trends (McKinley *et al* 2011). We computed trends for different periods within the time series, where the periods are all possible combinations of first and last years with time lengths $\geqslant$8 years within the time series (R package greenbrown version 2.4.3). Trends for each time period were computed from annually aggregated total burned area based on linear quantile regression to the median. Quantile regression is more robust than ordinary least squares regression because it reduces the effect of single extreme

years (i.e. years with extreme high burned area) on the estimated trend. Trend slopes were expressed as percentage of change relative to the multiyear mean of the time series. The two-tailed Mann-Kendall trend test was used to estimate the significance of the trends (Mann 1945, Kendall 1975). All analyses were done in the R software (R Core Team 2018) (an overview of the packages and functions used is provided in supplementary table 3).

2.3. Predictor data

Previous studies have identified a number of climatic variables, vegetation properties and socio-economic factors that either directly control or are surrogates for known mechanistic controls on fire occurrence and spread (Aldersley *et al* 2011, Bistinas *et al* 2014, Forkel *et al* 2017, 2019). For example, the number of wet days (WET) provides a measure of the average length of dry periods, while monthly maximum temperature (TMAX) and monthly diurnal temperature range (DTR) are measures of energetic constraints on fuel drying. Human population density (PD) has been widely used as a predictor of ignitions and/or fire suppression (Knorr *et al* 2014, Hantson *et al* 2015). The type of natural land cover (i.e. grassland, forest) influences both fuel availability and fire type. Measures such as vegetation greenness (i.e. fraction of absorbed photosynthetically active radiation, FAPAR) from optical satellite observations and vegetation optical depth (VOD) from microwave satellite observations provide measures of different changes in vegetation properties. Changes in FAPAR represent changes in green leaf cover and biomass (Myneni and Williams 1994) and hence FAPAR and related variables have been previously used as proxy for fuel loads in fire modelling (Pausas and Ribeiro 2013, Knorr *et al* 2014). VOD is proportional to the fuel moisture content (FMC) and aboveground biomass (BM) of vegetation (Jackson and Schmugge 1991, Sawada *et al* 2016):

$$VOD = b \times FMC \times BM$$

where b is a conversion factor that varies with vegetation type and depends on the frequency of microwaves (Griend and Wigneron 2004). Consequently, changes in VOD represent either changes in ecosystem biomass and/or fuel moisture content (Chaivaranont *et al* 2018, Fan *et al* 2018). Woody vegetation, mainly trees, dominate the above-ground biomass and total vegetation water content of an ecosystem. As a consequence, VOD is sensitive to changes in tree biomass (Liu *et al* 2013) and tree cover (Brandt *et al* 2017). Based on these sensitivities, FAPAR and VOD trends imply different changes in vegetation structure (Andela *et al* 2013) and hence might have different impacts on the estimation of burned area (Forkel *et al* 2017).

We used these climate, human population density, land cover and vegetation indices as input to the SOFIA model in order to assess changes in controls on fire. Climate data (WET, TMAX, DTR) were taken from the CRU TS3.2 dataset (Harris *et al* 2014). Human population density (PD) was taken from the global gridded data set of changes (Pesaresi *et al* 2013). Land cover was taken from the Land cover_CCI dataset (version 2.0.7, 1992–2015) (Li *et al* 2018). We translated land cover classes to the fractional coverage of plant functional types (PFT) per 0.25° grid cells using the cross-walking approach (Poulter *et al* 2015, Li *et al* 2016) with the conversion factors and PFT definitions as in Forkel *et al* (2017). The fractional coverage of PFTs was then aggregated to fractional coverage of trees, shrubs, herbaceous vegetation, and croplands. Vegetation changes were assessed by using FAPAR from the GIMMS3g dataset over the period 1982–2011 (Zhu *et al* 2013). VOD was obtained from a harmonized dataset of several passive microwave satellites over the period 1993–2012 (Liu *et al* 2011). Temporal gaps in both datasets were filled in two steps: firstly, by replacing seasonal (winter) gaps by the observed minimum value in each pixel and secondly, by filling remaining gaps with a smoothing spline.

2.4. SOFIA model

SOFIA is a generic model approach that allows the prediction of burned area using various model structures (Forkel *et al* 2017). In the version of the SOFIA model applied here, burned area (BA) was simulated on monthly time steps per 0.25° grid cells based on the fractional coverage of different land cover types (LC), and on controlling functions based on the predictors FAPAR, VOD, WET, TMAX, DTR and PD:

$$BA = \sum_{i=\{T,S,H,C\}} LC_i * f(FAPAR)_i * f(VOD)_i * f(WET)_i * f(TMAX)_i * f(DTR)_i * f(PD)$$

where T, S, H, and C are the fractional coverage of trees, shrubs, herbaceous vegetation, and croplands per 0.25° grid cells, respectively. FAPAR and VOD were used as average values over the 12 precedent months to account for the year-to-year variability in vegetation conditions.

The controlling functions f(x) are logistic functions:

$$f(x) = \frac{mx}{1 + e^{-sl \times (x - x0)}}$$

where the parameters mx, x0, and sl vary for each dataset x and by land cover type (Forkel *et al* 2017). Values of f(x) were trimmed to the range between zero (i.e. complete restriction of fire) and unity (complete allowance),

allowing the response functions to be represented as an exponential (supplementary figure 1 is available online at stacks.iop.org/ERC/1/051005/mmedia). The parameters of the controlling functions were estimated by optimizing the simulated monthly burned area from the SOFIA model against the GFED4 dataset for selected grid cells (supplement 1, supplementary table 1).

The SOFIA model simulations cover the period from 1994 (12 months after the beginning of the VOD dataset) until the end of 2011 (end of the FAPAR dataset). There were no harmonized long-term FAPAR and VOD datasets available that would allow us to run SOFIA simulations for the full periods of the GFED4 (1996–2015) or FireCCI50 (2001–2015) datasets.

The SOFIA model can be used to assess the relative contribution of a control x on the dynamics of burned area [BA(x)]:

$$BA(x) = \sum_{i=\{T,S,H,C\}} LC_i{}^{*}f(x)_i$$

This approach assumes that only a single factor x (e.g. FAPAR) controls burned area while all other factors have no effect on burning. In the following we refer to BA(x) as the 'marginal burned area'. We summed monthly BA and BA(x) time series to annual totals for the computation of trends. BA(x) time series are shown as anomalies relative to the average multiyear (1994–2011) total BA(x) for visual purposes in figure 2.

SOFIA reproduced global spatial patterns of burned area in comparison with the GFED4 and FireCCI50 burned area datasets but simulated global total burned area (295 Mha yr^{-1}) that is lower than the range from satellite datasets (supplementary figure 2). However, SOFIA reproduced the year-to-year variability and burned area trends within the uncertainties of the datasets in most regions (supplementary figures 3 and 4).

3. Variability in global burned area trends

We confirm previous studies that global burned area apparently declines over ~20 years (Andela *et al* 2017): The GFED4 and FireCCI50 datasets showed declining global burned area of $-0.74\%\ yr^{-2}$ between 1996–2015 and of $-0.66\%\ yr^{-2}$ between 2001–2015, respectively (figure 1). However, these trends are not significant. Furthermore, there is poor agreement in the trend shown by the GFED4 and FireCCI50 datasets for the period with overlap (2001–2015): The GFED4 dataset shows a stronger decline (factor 1.8, $-1.22\%\ yr^{-2}$) than the FireCCI50 dataset ($-0.66\%\ yr^{-2}$, figure 1(d)). Hence, the apparent decline in global burned area in GFED4 and FireCCI50 is not confirmed for the common period of these datasets.

The satellite data sets have a limited temporal coverage, and the identification of trends is strongly affected by years with abnormally high or low burned area at the beginning and end of the time series. In particular, the last three years 2013–2015 have very low global burned area and are the main cause of the reported decline over 1996/2001–2015 (figure 1(c)). On the other hand, 2011 had the largest global burned area in the FireCCI50 dataset and the third largest burned area in the GFED4 dataset and this would result in a plateau or a positive trend in burned area if the analysis were terminated in this year. The GFED4 dataset showed mostly significant declining trends ($p \leq 0.05$, Mann-Kendall trend test) if the first analysis year is between 1998 and 2002 and the last year is 2014 or 2015. The FireCCI50 dataset did not show a significant trend in global burned area for any sampled period (supplementary figure 3(b)). The estimated trend slopes for different time periods are not correlated ($r = 0.13$) between the two datasets (figure 1(d)).

Most of the overall decline in burned area occurs in northern-hemisphere Africa, southern-hemisphere South America, central Asia, and Australia, whereas large parts of southern-hemisphere Africa had increasing burned area (figure 1(a), supplementary figure 4). In general, the sign of the regional trends are consistent between the two sets of observations even though the slopes differ (figure 2). However, very few of the observed regional trends are significant.

The SOFIA model also shows a (non-significant) decline in global burned area between 1994 and 2011. Overall, the SOFIA model had mostly declining trends (figure 1(e)), especially if the first year of the analysis is before 2000 (supplementary figure 3(c)). In the period of overlap between the satellite observations and the simulation (2001–2011), there is agreement between the SOFIA model and the FireCCI50 dataset that there is no significant trend (or a slight positive tendency) in global burned area, whereas the GFED4 dataset shows a significant negative trend (figure 1(e), left panel). For the full period of each dataset and the common overlapping period, trends in simulated burned area from the SOFIA model are within the uncertainties of the satellite datasets.

The satellite datasets and the SOFIA model all show significant declining burned area in northern hemisphere Africa (figures 2(a), (f)). This region dominates the global decline in burned area. Southern-hemisphere Africa showed a tendency towards increasing burned area (figures 2(b), (g)). The FireCCI50 dataset and the SOFIA model had significant declining burned area in northern hemisphere South America (figure 2(h)). The satellite datasets suggest a non-significant decline and the SOFIA model a stable burned area in southern hemisphere South America (figures 2(d), (i)). The satellite datasets show a significant decline in burned

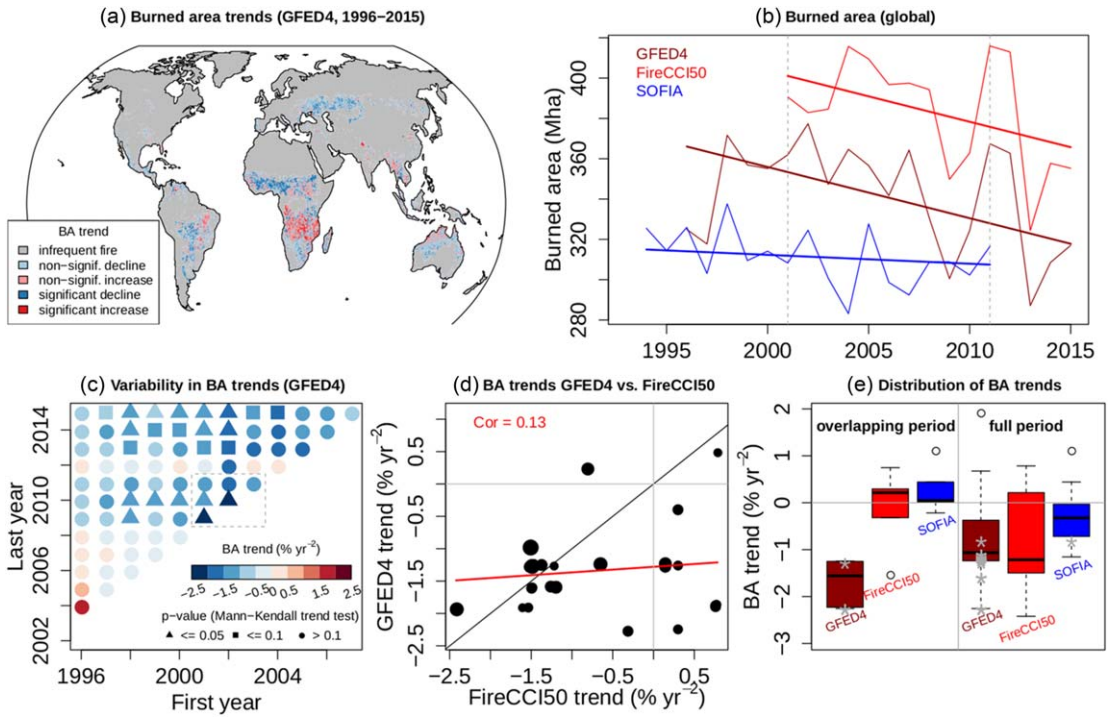

Figure 1. Variability in global burned area trends from satellite datasets and the SOFIA model. (a) Grid-cell level trends in annual burned area from the GFED4 dataset for the period 1996–2015. Trends were not computed in grid cells with infrequent fire (grey areas, i.e. BA $>$ 0 in less than 8 years). (b) Global annual total burned area and trends. None of the trends is significant. (c) Variability in the global burned area trend from the GFED4 dataset depending on the period (first to last year) for which the trend was calculated. Each point represents the global burned area trend slope as percentage to the mean global burned area for the period. Point symbols denote the significance according to the Mann-Kendall trend test. The grey rectangle highlights the overlapping period (2001–2011) of the two datasets and the SOFIA model. Supplementary figure 3 shows the same figure for the FireCCI50 dataset and the SOFIA model. (d) Comparison of the global burned area trend slope for different periods between the GFED4 and FireCCI50 datasets for periods of $\geq$ 8 years within 2001–2015. Larger points reflect trends based on longer periods (max 15 years). (e) Distribution of the global burned area trend slope from the GFED4 (i.e. the points from panel (c)), FireCCI50 datasets and the SOFIA model for the overlapping period (2001–2011) and for the full period of each dataset (GFED4: 1996–2015, FireCCI50: 2001–2015, SOFIA: 1994–2011). Significant trends are denoted with a grey-coloured * symbol ($p \leq 0.05$, Mann-Kendall trend test).

area in central Asia and Australia whereas the SOFIA model shows no trend in these regions (supplementary figure 4). In the following, controls on regional burned area trends will be assessed only for northern- and southern-hemisphere Africa and South America where trends are registered in satellite datasets and reproduced by SOFIA. The satellite datasets and the SOFIA model show a decline in global burned area overall but differences between the datasets prevent an accurate quantification of this decline.

4. Controls on regional burned area trends

The SOFIA simulations suggest that changes in climate, vegetation and human population had regionally diverse effects on marginal burned area and together shape the overall regional burned area trends (figure 2).

In northern-hemisphere Africa, the decline in burned area was driven by significant declines in the marginal burned area associated with population density, number of wet days and precedent FAPAR while maximum temperature caused a non-significant increase in the marginal burned area (figure 2(a)). According to the SOFIA model, increases in population density, wet days and FAPAR in tree-covered regions all cause a decline in burned area (supplementary figures 1(a), (c) and (d)). Thus, the positive trends in FAPAR ('greening') with a simultaneous increase in tree cover at the expense of herbaceous and shrub cover in northern-hemisphere Africa (supplementary figures 5 and 6), coupled with an increase in the number of wet days per month, and with increasing population density all contribute to reducing the amount of fire.

In southern-hemisphere Africa, however, the controls on burned area counteracted one another, resulting in no trend in simulated burned area. The marginal burned area declined because of increases in population density and number of wet days but increases in maximum temperature and VOD contributed to increasing marginal burned area (figure 2(b)). Strong positive trends in VOD occurred especially in regions dominated by herbaceous vegetation (supplementary figures 5 and 6). The fire-suppressing effects of increasing wetness and

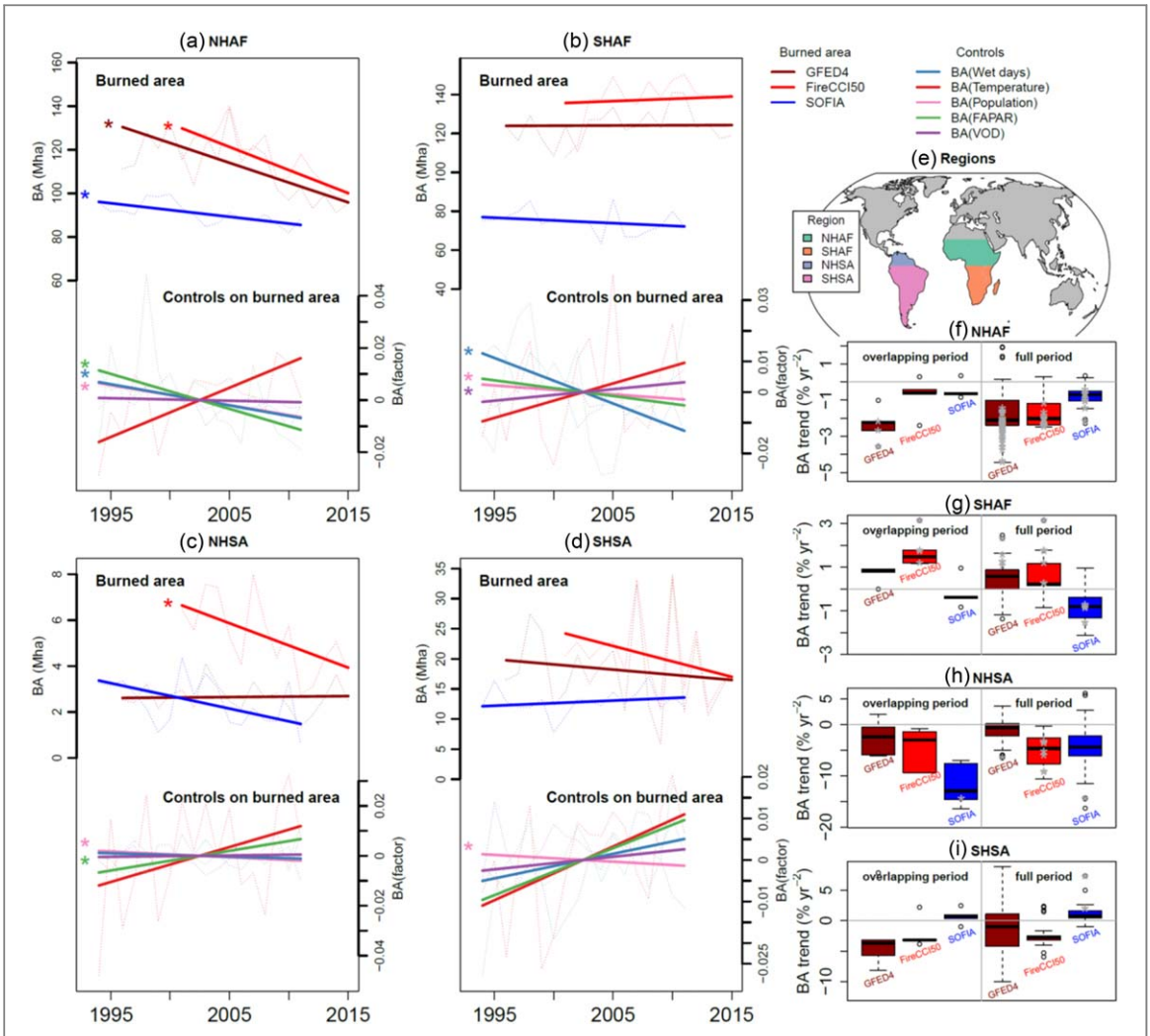

Figure 2. Trends and controls in regional burned area. Panels (a)–(d) show regional annual totals and trends of burned area (BA) and the marginal burned area, which is controlled by a single factor (BA(x) anomaly relative to mean BA(x) in 1994–2011). Trends denoted with a * star symbol are significant ($p \leq 0.05$, Mann-Kendall trend test). Panel (e) shows the spatial extent of the regions (NHAF = Northern-hemisphere Africa, SHAF = Southern-hemisphere Africa, NHSA = Northern-hemisphere South America, SHSA = Southern-hemisphere South America). Panels (f)–(i) show distributions of the regional burned area trend slope from the GFED4, FireCCI50 datasets and the SOFIA model for the overlapping period (2001–2011) and for the full period of each dataset. Results for other regions are shown in supplementary figure 4.

increasing population density compensate the tendency for increased burned area due to an increase in herbaceous fuels and temperature.

In both northern and southern hemisphere South America, population density contributed to declining marginal burned area and increasing temperatures and FAPAR contributed to increasing burned area (figures 2(c)–(d)). FAPAR had widespread positive trends especially in shrub or herbaceous-dominated regions (supplementary figure 5). Increasing FAPAR in non-tree-covered regions causes increasing marginal burned area in the SOFIA model (supplementary figure 1). In the arc of deforestation at the southern edge of the Amazon rainforests, VOD decreased because of decreasing tree cover (supplementary figure 5 and 6) (Andela *et al* 2013). This decrease in VOD caused an increase in the simulated marginal burned area (figure 2(d)). Hence, the SOFIA model results suggest that deforestation contribute to increased flammability in tropical forests. In summary, vegetation changes in South America are diverse but overall promote increasing burned area, which is then counteracted by changes in other factors.

5. Discussion and conclusions

Our results provide a more nuanced view of recent changes in global burned area. The multi-temporal trend analysis approach allows us to assess the robustness of trends by accounting for the effects of individual years. Although the satellite datasets do show a decline globally, we found that the decline is not significant, strongly affected by the year-to-year variability in burned area, mostly caused by the last three years (2013–2015) with low

global burned area, and shows major differences between satellite datasets. The detection of trends in (satellite) time series is generally hampered by changes in the underlying sensor (Tian *et al* 2015, Hammond *et al* 2018) and by the year-to-year variability and noise (Forkel *et al* 2013), which increases the number of years required to detect trends (Weatherhead *et al* 1998). Our results suggest that trends in burned area need to be examined with (1) longer and MODIS-independent satellite time series (e.g. by exploiting the AVHRR or Landsat archives); (2) with long-term regional observations (Kasischke and Turetsky 2006, Müller *et al* 2015, Doerr and Santín 2016); and (3) with independent fire-related variables (Kaiser *et al* 2012, Santín *et al* 2016).

Even with longer records, the interplay of climate, vegetation and human controls on fire will pose challenges for the attribution of the trends. Interpretations based on bivariate relationships only reflect the emergent controls on fire trends; attribution to fundamental underlying controls requires a more sophisticated approach using multivariate statistical or machine learning approaches (Bistinas *et al* 2014, Forkel *et al* 2019). Only by combining long time series and advanced analytical methods will it be possible to make robust statements about changes in fire regimes and the underlying controls.

The ability to reproduce recent trends in global burned area has been used as an indication of the poor performance of fire-enabled DGVMs (Andela *et al* 2017). This conclusion needs to be carefully re-assessed. DGVMs have regionally various performances in simulating burned area (Forkel *et al* 2019) and hence comparison of global trends might be misleading. Uncertainties in the satellite datasets also challenge the statement that 'fire models were unable to reproduce the pattern and magnitude of observed declines' (Andela *et al* 2017). The SOFIA model, in common with some of the fire-enabled DGVMs, has a weaker decline in global burned area (1994–2011) than the GFED4 dataset (1996–2015) but globally and in northern-hemisphere Africa it has comparable trends with the FireCCI50 dataset in the overlapping period.

As fire is influenced by the interplay of climate, vegetation, and human activities, changes in these controls can cause diverse changes in fire and burned area. The SOFIA model indicates that the decline in northern-hemisphere Africa is associated with increasing population density (Andela and van der Werf 2014, Andela *et al* 2017) but with an additional effect from increasing wetness. At the global scale, temperature and population density show positive and negative emergent relationships with burned area, respectively (Moritz *et al* 2012, Bistinas *et al* 2014, Knorr *et al* 2014, Forkel *et al* 2019). Our simulations with the SOFIA model show that the impacts of increases in population density and warming can counteract one another, resulting in weakened trends or stable burned area in many regions.

Changes in vegetation properties are important controls for regional trends in burned area. Northern-hemisphere Africa has experienced greening and increases in woody vegetation cover in recent decades (Fensholt *et al* 2013, Brandt *et al* 2017). Our results indicate that such a shift towards coarser fuels contributed to the decline in burned area because they have a dampening effect on fire (Kahiu and Hanan 2018). On the other hand, vegetation trends in grasslands in southern Africa (increasing VOD) and in forests in South America (decreasing VOD with increasing FAPAR) indicate increases in herbaceous biomass and reductions in woody vegetation cover (Andela *et al* 2013, Marle *et al* 2016) which promotes fire spread and contributes to positive trends in burned area. This is consistent with earlier findings that pasture burning increases burned area after deforestation in the Amazon (Cano-Crespo *et al* 2015). Hence our work confirms earlier observational and modelling studies (Krawchuk and Moritz 2011, Daniau *et al* 2012, Pausas and Ribeiro 2013, Kelley and Harrison 2014) suggesting that increased biomass leads to increased fire in fuel-limited regions but decreased fire in forests. Recent vegetation trends such as greening have contributed to observed changes in fire, but greening involves diverse changes in vegetation properties and thus produces complex though predictable impacts on burned area.

Our understanding of the role of vegetation changes in fire dynamics could certainly be improved with more data about fuel loads and fire-relevant plant traits and how these change with vegetation changes (Archibald *et al* 2018). To reduce the current uncertainty about future fire regimes (Settele *et al* 2014), large-scale, long-term, and temporally consistent datasets on fire and fire-relevant vegetation properties are the necessary prerequisite for an more informed development of global fire models.

Acknowledgments

We thank the following organisations, groups and researchers for providing datasets: GIMMS for FAPAR3g; the European Space Agency (ESA) for Fire_cci V50 and for Land cover_cci V2.0.7; the Global Fire Emissions Database consortium for the GFED4 burned area data; the Climate Research Unit for the CRU TS3.2 dataset; Y Liu for the VOD dataset. We thank A Arneth, M Forrest, M L Pettinari, M Thurner, G van der Werf, and C Yue for their comments on earlier versions of this manuscript. MF acknowledges support from ESA through a Living Planet Fellowship (4000116511/16/I-NB). MF, WD, and IT acknowledge support from the TU Wien-funded 'Wissenschaftspreis 2015', a personal science grant to WD. EC and AH received funding from the ESA Fire_cci

project. SPH acknowledges the support from the ERC-funded project GC2.0 (Global Change 2.0: Unlocking the past for a clearer future, grant number 694481).

ORCID iDs

Matthias Forkel https://orcid.org/0000-0003-0363-9697
Wouter Dorigo https://orcid.org/ttp://oi.og/0000-0001-8054-7572
Gitta Lasslop https://orcid.org/ttp://oi.og/0000-0001-9939-1459
Emilio Chuvieco https://orcid.org/ttp://oi.og/0000-0001-5618-4759
Stijn Hantson https://orcid.org/0000-0003-4607-9204
Irene Teubner https://orcid.org/ttp://oi.og/0000-0001-7916-5593
Kirsten Thonicke https://orcid.org/ttp://oi.og/0000-0001-5283-4937
Sandy P Harrison https://orcid.org/ttp://oi.og/0000-0001-5687-1903

References

Aldersley A, Murray S J and Cornell S E 2011 Global and regional analysis of climate and human drivers of wildfire *Sci. Total Environ.* **409** 3472–81
Andela N *et al* 2017 A human-driven decline in global burned area *Science* **356** 1356–62
Andela N, Liu Y Y, van Dijk A I J M, de Jeu R A M and McVicar T R 2013 Global changes in dryland vegetation dynamics (1988–2008) assessed by satellite remote sensing: comparing a new passive microwave vegetation density record with reflective greenness data *Biogeosciences* **10** 6657–76
Andela N and van der Werf G R 2014 Recent trends in African fires driven by cropland expansion and El Nino to La Nina transition *Nature Clim. Change* **4** 791–5
Archibald S *et al* 2018 Biological and geophysical feedbacks with fire in the Earth system *Environ. Res. Lett.* **13** 033003
Bistinas I, Harrison S P, Prentice I C and Pereira J M C 2014 Causal relationships versus emergent patterns in the global controls of fire frequency *Biogeosciences* **11** 5087–101
Bowman D M J *et al* 2009 Fire in the Earth System *Science* **324** 481–4
Bowman D M J S, Williamson G J, Abatzoglou J T, Kolden C A, Cochrane M A and Smith A M S 2017 Human exposure and sensitivity to globally extreme wildfire events *Nature Ecology & Evolution* **1**
Brandt M, Rasmussen K, Peñuelas J, Tian F, Schurgers G, Verger A, Mertz O, Palmer J R B and Fensholt R 2017 Human population growth offsets climate-driven increase in woody vegetation in sub-Saharan Africa *Nature Ecology & Evolution* **1**
Cano-Crespo A, Oliveira P J C, Boit A, Cardoso M and Thonicke K 2015 Forest edge burning in the Brazilian amazon promoted by escaping fires from managed pastures *J. Geophys. Res. Biogeosci.* **120** 2015JG002914
Chaivaranont W, Evans J P, Liu Y Y and Sharples J J 2018 Estimating grassland curing with remotely sensed data *Nat. Hazards Earth Syst. Sci.* **18** 1535–54
Chuvieco E *et al* 2018 Generation and analysis of a new global burned area product based on MODIS 250 m reflectance bands and thermal anomalies *Earth System Science Data* **10** 2015–31
Chuvieco E, Yue C, Heil A, Mouillot F, Alonso-Canas I, Padilla M, Pereira J M, Oom D and Tansey K 2016 A new global burned area product for climate assessment of fire impacts *Global Ecol. Biogeogr.* **25** 619–29
Cruz M G, Sullivan A L, Gould J S, Sims N C, Bannister A J, Hollis J J and Hurley R J 2012 Anatomy of a catastrophic wildfire: the black saturday kilmore east fire in Victoria, Australia *Forest Ecology and Management* **284** 269–85
Daniau A-L *et al* 2012 Predictability of biomass burning in response to climate changes *Global Biogeochem. Cycles* **26** GB4007
Dennison P E, Brewer S C, Arnold J D and Moritz M A 2014 Large wildfire trends in the western United States, 1984–2011 *Geophys. Res. Lett.* **41** 2014GL059576
Doerr S H and Santín C 2016 Global trends in wildfire and its impacts: perceptions versus realities in a changing world *Phil. Trans. R. Soc.* B **371** 20150345
Fan L *et al* 2018 Evaluation of microwave remote sensing for monitoring live fuel moisture content in the mediterranean region *Remote Sens. Environ.* **205** 210–23
Fensholt R, Rasmussen K, Kaspersen P, Huber S, Horion S and Swinnen E 2013 Assessing land degradation/recovery in the african sahel from long-term earth observation based primary productivity and precipitation relationships *Remote Sensing* **5** 664–86
Forkel M *et al* 2019 Emergent relationships with respect to burned area in global satellite observations and fire-enabled vegetation models *Biogeosciences* **16** 57–76
Forkel M, Carvalhais N, Verbesselt J, Mahecha M, Neigh C and Reichstein M 2013 Trend change detection in NDVI time series: effects of inter-annual variability and methodology *Remote Sensing* **5** 2113–44
Forkel M, Dorigo W, Lasslop G, Teubner I, Chuvieco E and Thonicke K 2017 A data-driven approach to identify controls on global fire activity from satellite and climate observations (SOFIA V1) *Geosci. Model Dev.* **10** 4443–76
Giglio L, Boschetti L, Roy D P, Humber M L and Justice C O 2018 The collection 6 MODIS burned area mapping algorithm and product *Remote Sens. Environ.* **217** 72–85
Giglio L, Randerson J T and van der Werf G R 2013 Analysis of daily, monthly, and annual burned area using the fourth-generation global fire emissions database (GFED4) *J. Geophys. Res. Biogeosci.* **118** 317–28
Griend A A V de and Wigneron J P 2004 The b-factor as a function of frequency and canopy type at H-polarization *IEEE Trans. Geosci. Remote Sens.* **42** 786–94
Hammond M L, Beaulieu C, Henson S A and Sahu S K 2018 Assessing the presence of discontinuities in the ocean color satellite record and their effects on chlorophyll trends and their uncertainties *Geophys. Res. Lett.* **45** 7654–62
Hantson S *et al* 2016 The status and challenge of global fire modelling *Biogeosciences* **13** 3359–75
Hantson S, Lasslop G, Kloster S and Chuvieco E 2015 Anthropogenic effects on global mean fire size *Int. J. Wildland Fire* **24** 589–96
Harris I, Jones P D, Osborn T J and Lister D H 2014 Updated high-resolution grids of monthly climatic observations—the CRU TS3.10 dataset *Int. J. Climatol.* **34** 623–42

Holden Z A, Swanson A, Luce C H, Jolly W M, Maneta M, Oyler J W, Warren D A, Parsons R and Affleck D 2018 Decreasing fire season precipitation increased recent western US forest wildfire activity *PNAS* **115** 201802316
Humber M L, Boschetti L, Giglio L and Justice C O 2019 Spatial and temporal intercomparison of four global burned area products *Int. J. Digital Earth* **12** 460–484
Jackson T J and Schmugge T J 1991 Vegetation effects on the microwave emission of soils *Remote Sens. Environ.* **36** 203–12
Jolly W M, Cochrane M A, Freeborn P H, Holden Z A, Brown T J, Williamson G J and Bowman D M J S 2015 Climate-induced variations in global wildfire danger from 1979 to 2013 *Nat. Commun.* **6** 7537
Kahiu M N and Hanan N P 2018 Fire in sub-Saharan Africa: the fuel, cure and connectivity hypothesis *Global Ecol. Biogeogr.* **27** 946–57
Kaiser J W *et al* 2012 Biomass burning emissions estimated with a global fire assimilation system based on observed fire radiative power *Biogeosciences* **9** 527–54
Kasischke E S and Turetsky M R 2006 Recent changes in the fire regime across the North American boreal region—spatial and temporal patterns of burning across Canada and Alaska *Geophys. Res. Lett.* **33** L09703
Kelley D I and Harrison S P 2014 Enhanced Australian carbon sink despite increased wildfire during the 21st century *Environ. Res. Lett.* **9** 104015
Kendall M G 1975 *Rank Correlation Methods* (London: Griffin)
Knorr W, Kaminski T, Arneth A and Weber U 2014 Impact of human population density on fire frequency at the global scale *Biogeosciences* **11** 1085–102
Krawchuk M A and Moritz M A 2011 Constraints on global fire activity vary across a resource gradient *Ecology* **92** 121–32
Krawchuk M A, Moritz M A, Parisien M-A, Dorn J V and Hayhoe K 2009 Global pyrogeography: the current and future distribution of wildfire *PLoS One* **4** e5102
Li W, Ciais P, MacBean N, Peng S, Defourny P and Bontemps S 2016 Major forest changes and land cover transitions based on plant functional types derived from the ESA CCI Land Cover product *Int. J. Appl. Earth Obs. Geoinf.* **47** 30–9
Li W, MacBean N, Ciais P, Defourny P, Lamarche C, Bontemps S, Houghton R A and Peng S 2018 Gross and net land cover changes in the main plant functional types derived from the annual ESA CCI land cover maps (1992–2015) *Earth System Science Data* **10** 219–34
Liu Y Y, van Dijk A I J M, de Jeu R A M, Canadell J G, McCabe M F, Evans J P and Wang G 2015 Recent reversal in loss of global terrestrial biomass *Nature Clim. Change* **5** 470–4
Liu Y Y, van Dijk A I J M, McCabe M F, Evans J P and de Jeu R A M 2013 Global vegetation biomass change (1988–2008) and attribution to environmental and human drivers *Global Ecol. Biogeogr.* **22** 692–705
Liu Y Y, de Jeu R A M, McCabe M F, Evans J P and van Dijk A I J M 2011 Global long-term passive microwave satellite-based retrievals of vegetation optical depth *Geophys. Res. Lett.* **38** L18402
Mann H B 1945 Nonparametric tests against trend *Econometrica* **13** 245–59
Marle M J E van, Werf G R van der, Jeu R A M de and Liu Y Y 2016 Annual South American forest loss estimates based on passive microwave remote sensing (1990–2010) *Biogeosciences* **13** 609–24
McKinley G A, Fay A R, Takahashi T and Metzl N 2011 Convergence of atmospheric and North Atlantic carbon dioxide trends on multidecadal timescales *Nature Geosci* **4** 606–10
Moritz M A, Parisien M-A, Batllori E, Krawchuk M A, Van Dorn J, Ganz D J and Hayhoe K 2012 Climate change and disruptions to global fire activity *Ecosphere* **3** 1–22
Müller M, Vacik H and Valese E 2015 Anomalies of the Austrian forest fire regime in comparison with other alpine countries: a research note *Forests* **6** 903–13
Myneni R B and Williams D L 1994 On the relationship between FAPAR and NDVI *Remote Sens. Environ.* **49** 200–11
Pausas J G and Ribeiro E 2013 The global fire–productivity relationship *Global Ecol. Biogeogr.* **22** 728–36
Pesaresi M *et al* 2013 A global human settlement layer from optical HR/VHR RS data: concept and first results *IEEE Journal of Selected Topics in Applied Earth Observations and Remote Sensing* **6** 2102–31
Poulter B *et al* 2015 Plant functional type classification for earth system models: results from the European space agency's land cover climate change initiative *Geosci. Model Dev.* **8** 2315–28
R Core Team 2018 *R: A Language and Environment for Statistical Computing* (Vienna, Austria: R Foundation for Statistical Computing) Online:https://R-project.org/
Santín C, Doerr S H, Kane E S, Masiello C A, Ohlson M, Rosa J M de la, Preston C M and Dittmar T 2016 Towards a global assessment of pyrogenic carbon from vegetation fires *Global Change Biol.* **22** 76–91
Sawada Y, Tsutsui H, Koike T, Rasmy M, Seto R and Fujii H 2016 A field verification of an algorithm for retrieving vegetation water content from passive microwave observations *IEEE Trans. Geosci. Remote Sens.* **54** 2082–95
Settele J, Scholes R J, Betts R, Bunn S, Leadley P, Nepstad D C, Overpeck J T and Taboada M A 2014 Terrestrial and Inland water systems *Climate Change 2014—Impacts, Adaptation and Vulnerability: Part A: Global and Sectoral Aspects: Working Group II Contribution to the IPCC Fifth Assessment Report: Volume 1: Global and Sectoral Aspects* 1 Intergovernmental Panel on Climate Change (Cambridge: Cambridge University Press) pp 271–360 Online:https://cambridge.org/core/books/climate-change-2014-impacts-adaptation-and-vulnerability-part-a-global-and-sectoral-aspects/terrestrial-and-inland-water-systems/CCE23ED790D400923D800C963618F2EC
Stephens S L *et al* 2014 Temperate and boreal forest mega-fires: characteristics and challenges *Frontiers in Ecology and the Environment* **12** 115–22
Tian F, Fensholt R, Verbesselt J, Grogan K, Horion S and Wang Y 2015 Evaluating temporal consistency of long-term global NDVI datasets for trend analysis *Remote Sens. Environ.* **163** 326–40
Turco M, Rosa-Cánovas J J, Bedia J, Jerez S, Montávez J P, Llasat M C and Provenzale A 2018 Exacerbated fires in Mediterranean Europe due to anthropogenic warming projected with non-stationary climate-fire models *Nat. Commun.* **9** 3821
Van Lierop P, Lindquist E, Sathyapala S and Franceschini G 2015 Global forest area disturbance from fire, insect pests, diseases and severe weather events *Forest Ecology and Management* **352** 78–88
Weatherhead E C *et al* 1998 Factors affecting the detection of trends: statistical considerations and applications to environmental data *Journal of Geophysical Research: Atmospheres* **103** 17149–61
Zhu Z *et al* 2016 Greening of the Earth and its drivers *Nat. Clim. Change* **6** 791–5
Zhu Z, Bi J, Pan Y, Ganguly S, Anav A, Xu L, Samanta A, Piao S, Nemani R and Myneni R 2013 Global data sets of vegetation leaf area index (LAI)3g and fraction of photosynthetically active radiation (FPAR)3g derived from global inventory modeling and mapping studies (GIMMS) normalized difference vegetation index (NDVI3g) for the period 1981 to 2011 *Remote Sensing* **5** 927–948